NASA Technical Memorandum 107365

Experimental Visualization of Flows in Packed Beds of Spheres

R.C. Hendricks
Lewis Research Center
Cleveland, Ohio

S. Lattime
B&C Engineering
Akron, Ohio

M.J. Braun
University of Akron
Akron, Ohio

M.M. Athavale
CFD Research Corporation
Huntsville, Alabama

Prepared for the
First Pacific Symposium on Flow Visualization and Image Processing
sponsored by the Pacific Center of Thermal-Fluids Engineering
Honolulu, Hawaii, February 23–26, 1997

National Aeronautics and
Space Administration

EXPERIMENTAL VISUALIZATION OF FLOWS IN PACKED BEDS OF SPHERES

R.C. Hendricks
NASA Lewis Research Center
Cleveland, Ohio 44135, USA

S. Lattime
B& C Engineering
Akron, Ohio 44325, USA

M.J. Braun
University Of Akron
Akron, Ohio 44325, USA

M.M. Athavale
CFD Research Corp
Huntsville, Alabama 35805, USA

ABSTRACT

The flow experiment consisted of an oil tunnel , 76 × 76 mm in cross-section, packed with lucite spheres. The index of refraction of the working fluid and the spheres were matched such that the physical spheres invisible to the eye and camera. By seeding the oil and illuminating the packed bed with planar laser light sheet, aligned in the direction of the bulk flow, the system fluid dynamics becomes visible and the 2-D projection was recorded at right angles to the bulk flow. The planar light sheet was traversed from one side of the tunnel to the other providing a simulated 3-D image of the entire flow field. The boundary interface between the working fluid and the sphere rendered the sphere black permitting visualization of the exact locations of the circular interfaces in both the axial and transverse directions with direct visualization of the complex interstitial spaces between the spheres within the bed. Flows were observed near the surfaces of a plane and set of spheres as well as minor circles that appear with great circles and not always uniformly ordered. In addition to visualizing a very complex flow field, it was observed that flow channeling in the direction of the bulk flow occurs between sets of adjacent spheres. Still photographs and video recordings illustrating the flow phenomena will be presented.

INTRODUCTION

Packed spherical particle beds are usual characterized by an empirical combination of laminar and turbulent flows, the Ergun (1952) relations as demonstrated by Bird et al. (1960) are probably the best known. These relations enable process designers to fabricate devices with packed beds of spheres for a wide variety of applications including porous media, catalytic packs, heaters, and heat exchangers yet little is known of the details of heat, mass and momentum transfer in these packed structures. Jolls and Hanratty (1966) studied a sphere in a dumped bed of spheres. For Reynolds numbers less than 40, the flow field was 3-D laminar with unsteady flows occurring 110 < Re < 150. These results were confirmed by Karabelas (1970). Wenger et al. (1971) investigated the flow about a sphere in a close packed cubic array of spheres. Steady flow exists to Re = 82, and characterized by nine regions of reverse flow with the same type of flows observed for Re = 200 even though the flow is now unsteady. Saleh et al. (1992), Rosenstein (1980), Yarlagadda (1989), indicated that while progress was being made in numerical modeling of porous media, little knowledge of the interstitial flow fields is available. Saleh presents a study performed in a porous media using a particle image displacement velocimetry to determine the velocity in a planar field while the third velocity can be derived from the integration of the continuity equation. The concept on concomitant determination of all three velocities is similar to that of Rosenstein.

Herein the Full Flow Field Tracking (FFFT) method (Braun et al. 1988, 1990) will be applied to visualize and quantize the flow patterns and fluid velocities within a packed bed of spheres.

TEST FACILITY

The test facility consisted of a tunnel, flow system, video equipment, laser, lens systems, and data recorders and a test configuration, Figs. 1 and 2. The matrix of spheres represented schematically in Fig. 3, was fabricated to fill the cross section of an aluminum tunnel (1524 × 76.2 × 76.2 mm) with lucite wall test section. Two such matrices were fabricated using optical glue to bind the array having the same index of refraction as the lucite, 1.4905. This technique allows a clear view through the spheres even at their points of contact when immersed in a fluid with the same index of refraction. The bottom layer of spheres were ground flat with the tunnel floor and the height adjusted to exactly fit the

tunnel. The width was adjusted using a ramp that blocked a portion of the tunnel. The spheres are arranged in a staggered manner, and numbered for reference and to facilitate flow descriptions.

The first packed sphere bed (78.7 mm long × 50.8 mm wide × 76.2 mm height) contains a 7 × 7 longitudinal array, Fig. 4(a), with a transverse array of four, Fig. 4(b), 12.7 mm diameter spheres, for a total of 172 spheres, Fig. 4(c). The volume of the test array is Vt = 18.6 in.^{3}, the solid volume is Vs =11.25 in.^{3} with the void being the difference, Vo = 7.35 in.^{3} with an effective open cross section of Ae = 1.09 in.^{2}

The second packed sphere bed contains a 5-long × 4.5-height × 3-wide array, a total of 67.5 spheres, 19.05 mm diameter, and ground to fit exactly into the tunnel. The volume of the test array is Vt= 20.4 in.^{3} with Vs = 12.7 in.^{3} and the void Vo= 7.7in.^{3} The effective open cross sectional area is Ae = 0.917in.^{2} We will not report data for this array in this paper.

The coherent beam 5CW argon-ion laser was directed through an optical train with micrometrically adjustable mirrors and passes through two cylindrical lenses positioned at 90° with respect to each other, through the lucite windows and into the tunnel. This system produces a sheet of light approximately 1 mm thickness from the first lens and 0.1 mm thickness from the second lens. To provide illumination, the flow was seeded with magnesium oxide to provide flow tracers. The micrometric adjustments controls the scanning process during which light slices of the test section were obtained and assembled via video recording at 30 Hz to provide a 3-D visualization of the flow field, Fig. 2.

Finally, four static pressure taps upstream and downstream of the test matrix provide the bulk pressure drop and inlet and outlet thermocouples monitor the bulk temperature rise of the fluid.

CALIBRATION

The dimensional and time scales provide an implicit velocity scale. The dimensional scales were established using grid lines with a 3.9X magnification for general viewing and 7.8X for close-up details. The time scale is delivered by the camera; the screen is laced with two fields each 1/60 sec producing a frame every 1/30 sec. The use of a strobe light provides a method of segmented flow streaks enabling a more accurate determination of the velocity of the tracer streak.

RESULTS

Figure 5 represents the flow field in the 12.7 mm diameter array of spheres, when the flow is 1 GPM. The laser light slice is 6.35 mm (z = 1.0) from the front lateral wall; the image was strobed at 180 Hz, hence there are six segments to the particle streak. Spheres 1 to 4 represent the first column and the flow streaks resemble those about a pinned cylindrical array. Stagnation zones are seen in front of spheres 1 to 4 while wake zones appear behind spheres 22 to 25. Flow in the first row below the tunnel top surface, spheres 4 to 11 and 18 to 25, exhibits a high level of distortion from flow symmetry; lower velocities as evidenced by the closely dotted streaks illustrate the profound influence of a sphere-wall boundary. Careful attention to the particle trace lengths and brightness defines a flow thread in the axial direction. In regular arrays the flow thread trajectory resembles a complex sine wave; in Fig. 5, the flow spirals upward from the gap between spheres 16 to 20, is slowed and turned downward by the sphere residing in the pocket formed by spheres 16 to 19 and 20 to 23 and exits between spheres 20 to 23. The streak between spheres 1 to 2 is seen heading for the stagnation zone of sphere-5; the wake of sphere-5 is vivid and a streak extends toward, but downward from the stagnation zone of sphere-12. The wake behind sphere 14 and the stagnation region in front of sphere 21 are almost connected, but are disjoint illustrating the complexity of the flow thread.

Figure 6 presents flow details between spheres in the first and second columns of the matrix. Stagnation points in front of spheres 2 and 3 and the boundary layers around spheres 9 and 10 can be seen. Closing of small wakes behind spheres 2 and 3 are readily observed.

Figure 7 illustrates the flow mid way across the tunnel, 25.4 mm from the front wall (z = 4). The effects of the wall on the flow between spheres 11 to 14 and 18 to 21 are pronounced; especially notice the diminished velocities in the region between spheres 11 to 18 and the wall. The seeming lines of flow symmetry between spheres 13 to 14 and 17 to 18 are well delineated.

Figure 8 illustrates flow in the last two columns of spheres (6 to 7). Note the boundary layer effects in Fig. 8(a) underside of sphere 21 to 18, and the wake behind sphere-25. The jet emerging between the wall and the back side of sphere-25 is pushing the wake region slightly off centerline of the sphere; note, however that sphere-25 has no downstream sphere to influence the flow. In Fig. 8(b), the wake behind sphere-24 is strong and the accelerated flows show behind sphere-20.

At 3 GPM, the boundary layers, jetting, and wakes become more prominent. Figure 9 provides a transverse scan the at the column of spheres 5 to 7 axial location. Figure 9(a) shows the flow in the immediate vicinity of the front lateral wall (z = 0). The flow patterns about the half-sphere and the resemblance of the flow thread are quite prominent. Figure 9(b) illustrates the flows at z = 1.0 (6.4 mm) and the particle tracking the flow thread wave is partially obscured. In Fig. 9(c) at z = 2 (12.7 mm), a portion of the adjacent spheres are visible as are the multiple contact points, while Fig. 9(d), z = 3 (29.1 mm) shows the flow streak and contact points.

Figure 10 presents a closeup at 7.8X, of the flow in the same longitudinal plane as that of Fig. 10 at 12.7 mm (z = 2) from the front wall. One notices here the strong nature of a lazy 3-D flow with a stagnation region in the cusp indicated at the confluence between the spheres shown in the drawing of Fig. 3 and a very slow flow in the channel between the spheres.

VIDEO

The visualization of the flow fields is available in 1/2-in. VHS format. This video provides a scan of the flow field from front to rear lateral walls illustrating details of the flow boundary layer close to the wall and progressing through the matrix to the opposite wall. The flow details illustrate the flow threads in

the lateral direction or direction of the bulk flow. The video is also used to determine quantitative information as the flow velocities using the FFFT technique.

SUMMARY

A set of experiments designed to determine the qualitative and quantitative nature of flow in matrices of spheres, where the spheres are arranged in a staggered fashion. It has been found that for the Reynolds numbers used in these experiments, which were relatively low, the flow had in general a structure similar to that of a laminar flow, and for the 1 GPM case it even resembled the structure of potential flow. The change in the size of the spheres of the matrix did not bring any qualitative changes to the flow. It has been determined that the flow has a strong three dimensional characteristics, even at low velocities. Nevertheless, the FFFT technique used in this experiment was able to successfully follow the flow for short periods of times in two-dimensional planes.

The 1/2 VHS video tape presents the 3-D time dependent character of the flow within the matrix of spheres. The tape can be used extensively in the process of validation studies.

REFERENCES

1. Bird, R.B., Stewart, W.E., and Lightfoot, E.N. (1960), Transport Phenomena, John Wiley Press, New York, p. 200.
2. Braun, M.J., Batur, C., Karavelakis, G. (1988) "Digital Image Processing Through Full Flow Field Tracing (FFFT) in Narrow Geometries at Low Reynolds Numbers," First National Fluid Dynamics Congress, Cincinnati, Ohio, July 24–28.
3. Braun, M.J., Hendricks, R.C., and Canacci, V.A. (1990) A "Flow Visualization in a Simulated Brush Seal," Paper 90–GT–217, 35 ASME Int. Gas Turbine and Aero-engine Congress and Exposition, June 11-14, Brussels, Belgium.
4. Egrun, S. (1952), Chem. Engr. Prog. 43 (93).
5. Jolls, K.R., Hanratty, T.J., (1966) Chemical Engineering Science, Vol. 21, pp. 1185.
6. Karabelas, A.J. (1970) PhD Thesis, Chemical Engineering, University of Illinois, Urbana.
7. Rosenstein, H.D., (1980) "Nonlinear Laminar Flow in a Porous Medium," PhD. Thesis, Case Western Reserve University.
8. Saleh, S., Thovert, J.F., Adler, P.M. (1992) "Measurement of Two-Dimensional Velocity Fields in Porous Media by Particle Image Displacement Velocimetry." Experiments in Fluids, Vol. 12, pp. 210–212.
9. Wegner, T.H., Karabelas, A.J., Hanratty, T.J. (1971) "Visual Studies in a Regular Array of Spheres," Chemical Engineering Science, Vol. 26, pp. 59–63.
10. Yarlagadda, A.P., Yoganathan, A.P. (1989) "Experimental Studies of Model Porous Media Fluid Dynamics," Experimental Fluids, Vol. 8, pp. 59–71.

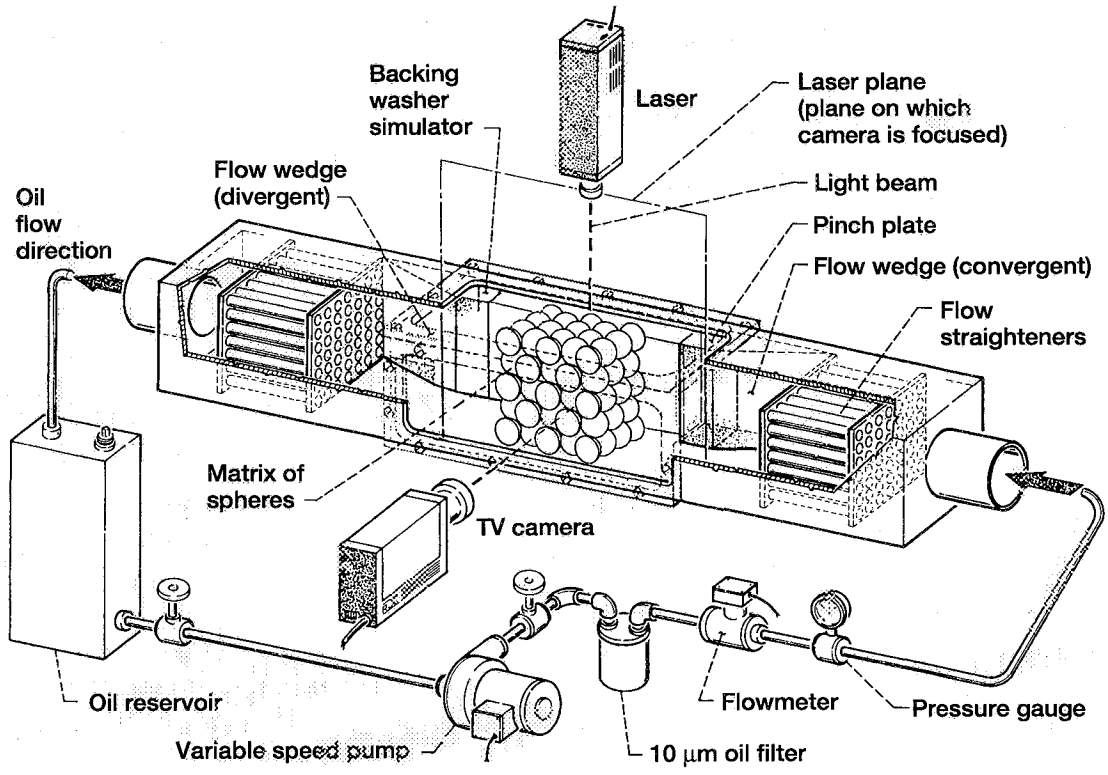

Figure 1.—Schematic of the Test Facility.

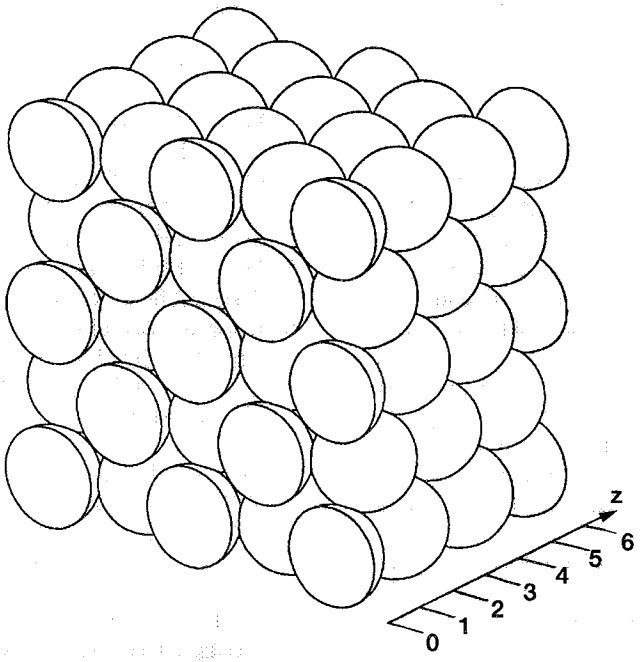

Figure 2.—Schematic of a matrix of spheres.The planes of the light sheet are indicated at z = 0 (front wall); z = 1 (6.4 mm); z = 2 (12.7 mm); z = 3 (19.1 mm); z = 4 (midplane);

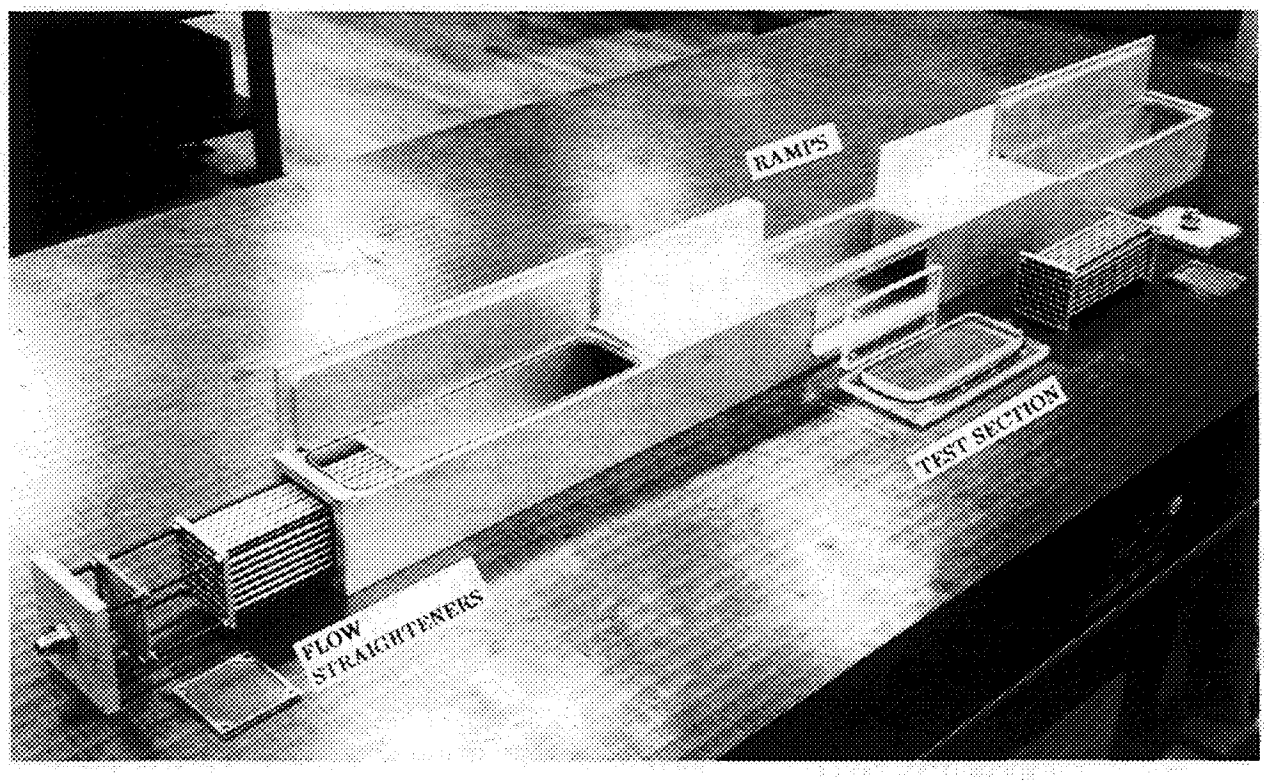

Figure 3.—Oil tunnel and its components.

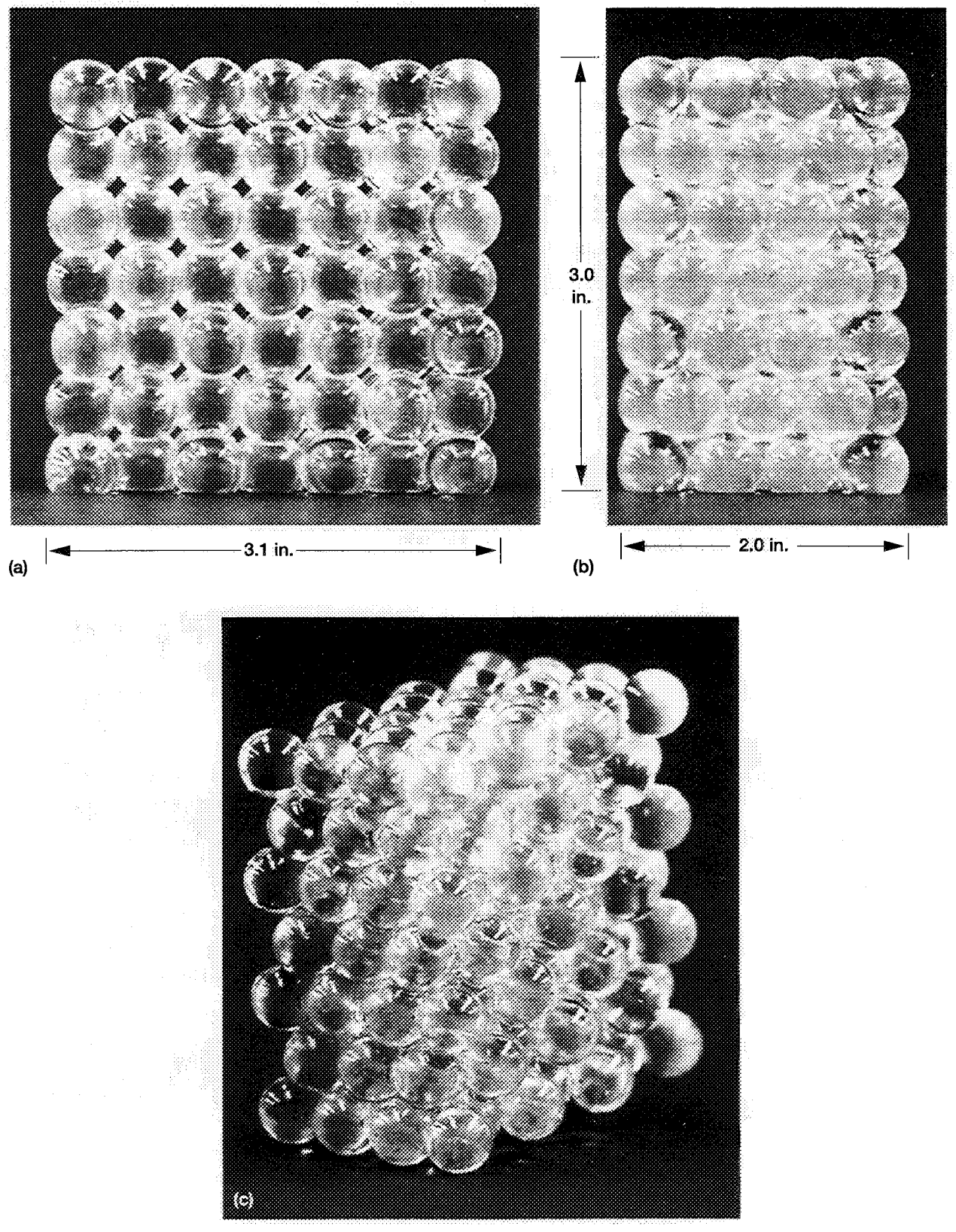

Figure 4.—Matrices of lucite spheres of refractive index RI = 1.4900; sphere diameter = 12.7 mm.

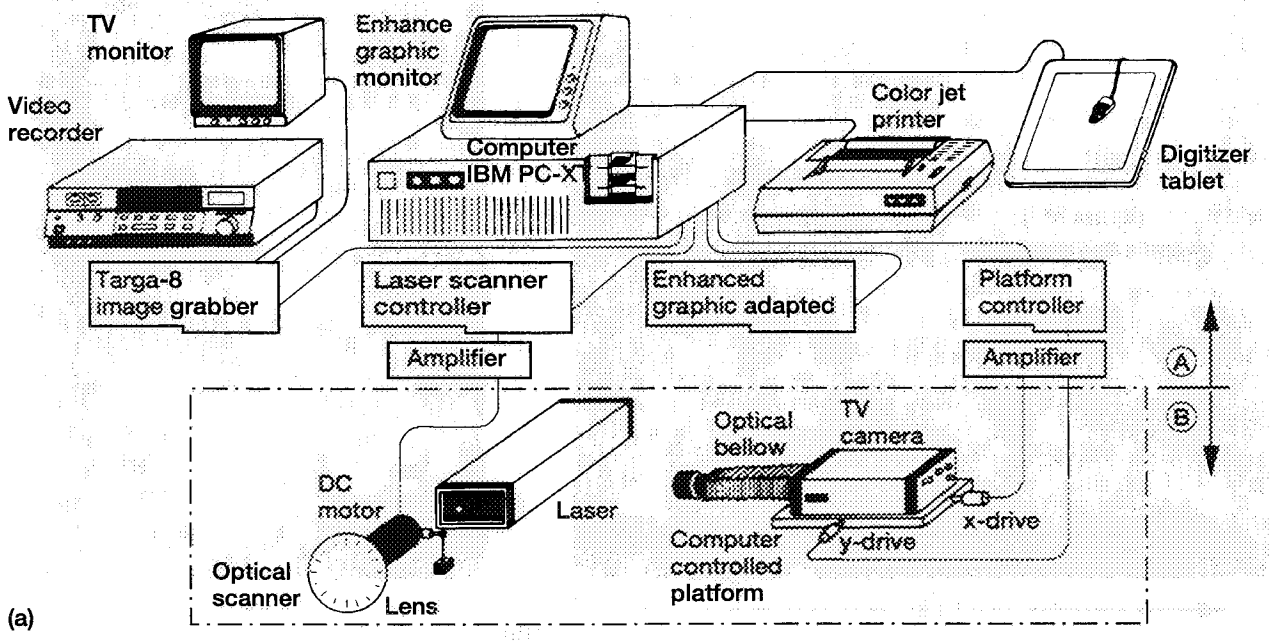

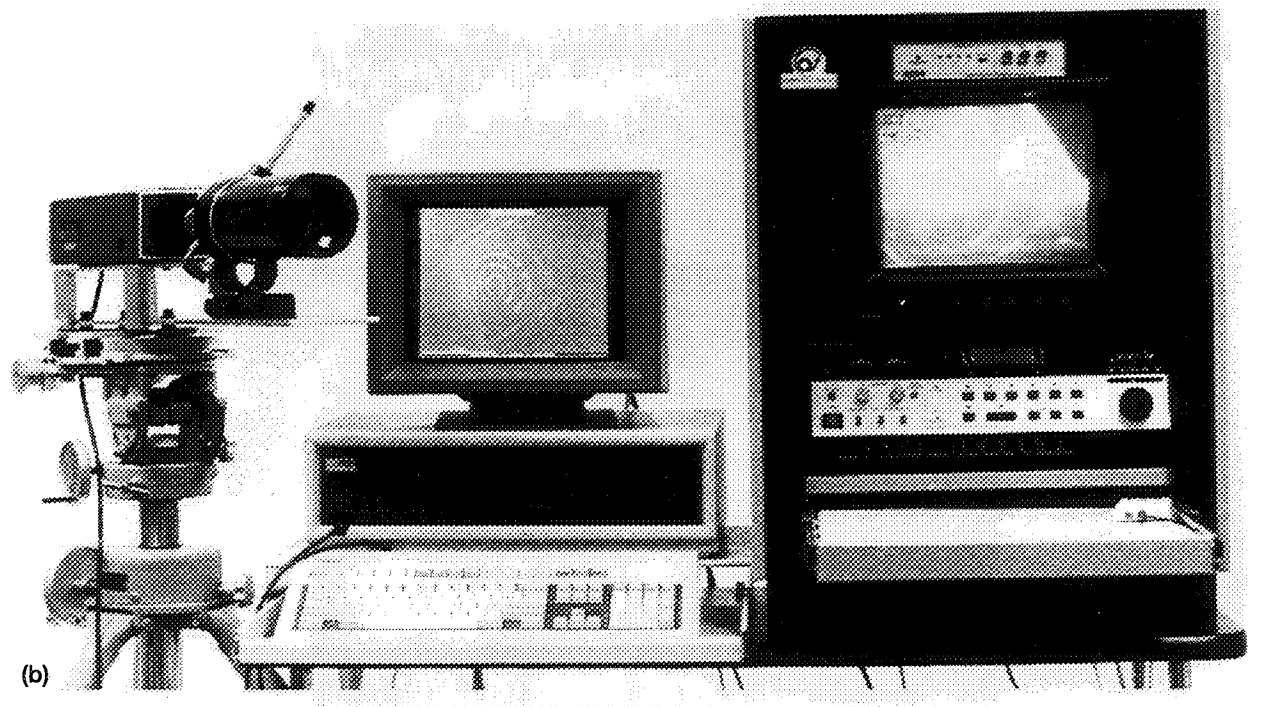

Figure 5.—Schematic of image and processing system. (a) Schematic of image processing system. (b) Photograph of Imaging system.

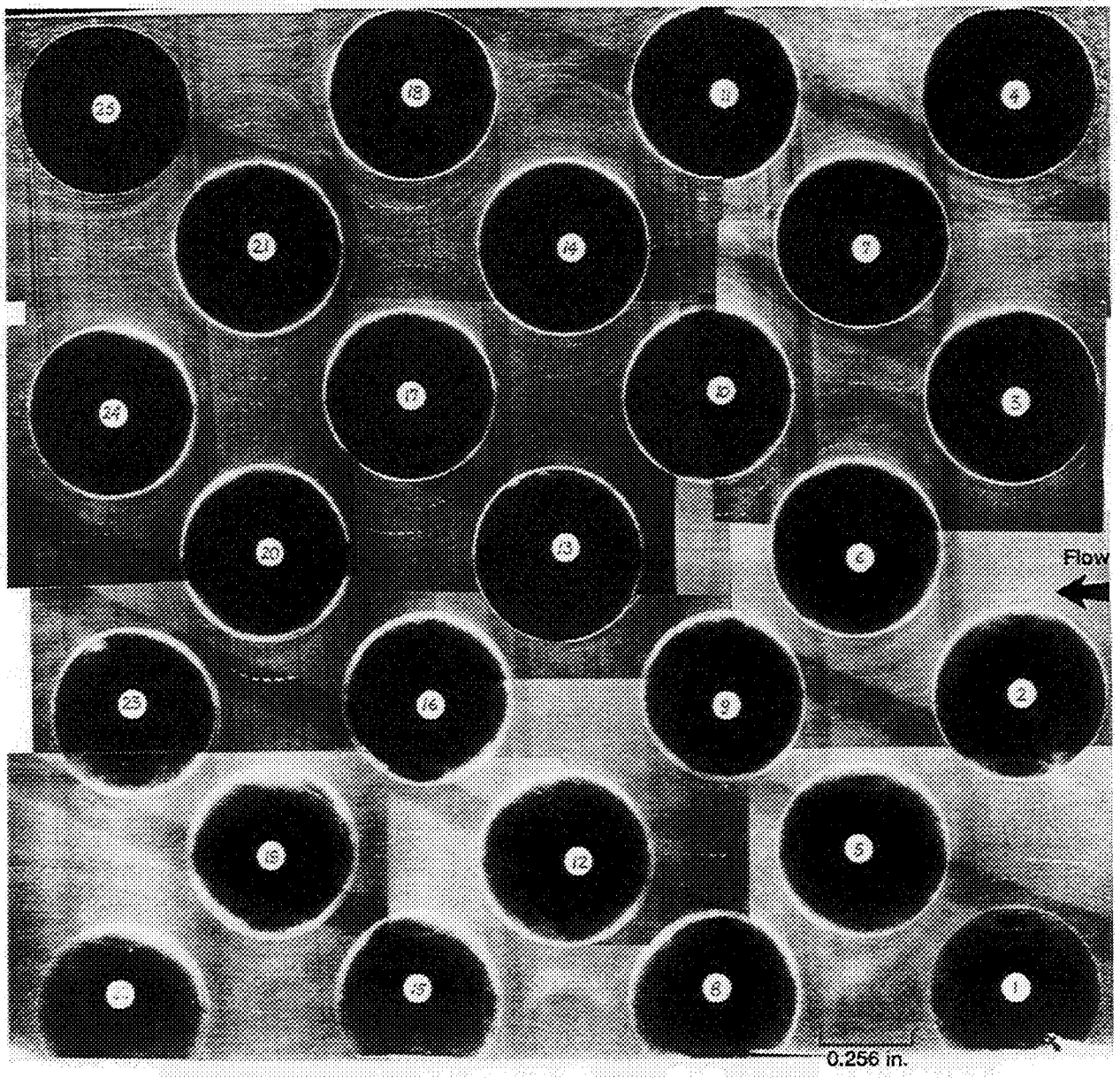

Figure 6.—Visualization of flow in a 12.7 mm diameter sphere matrix (figure 4), 6.4 mm from front wall (z = 1.0); flow at 1.0 GPM.

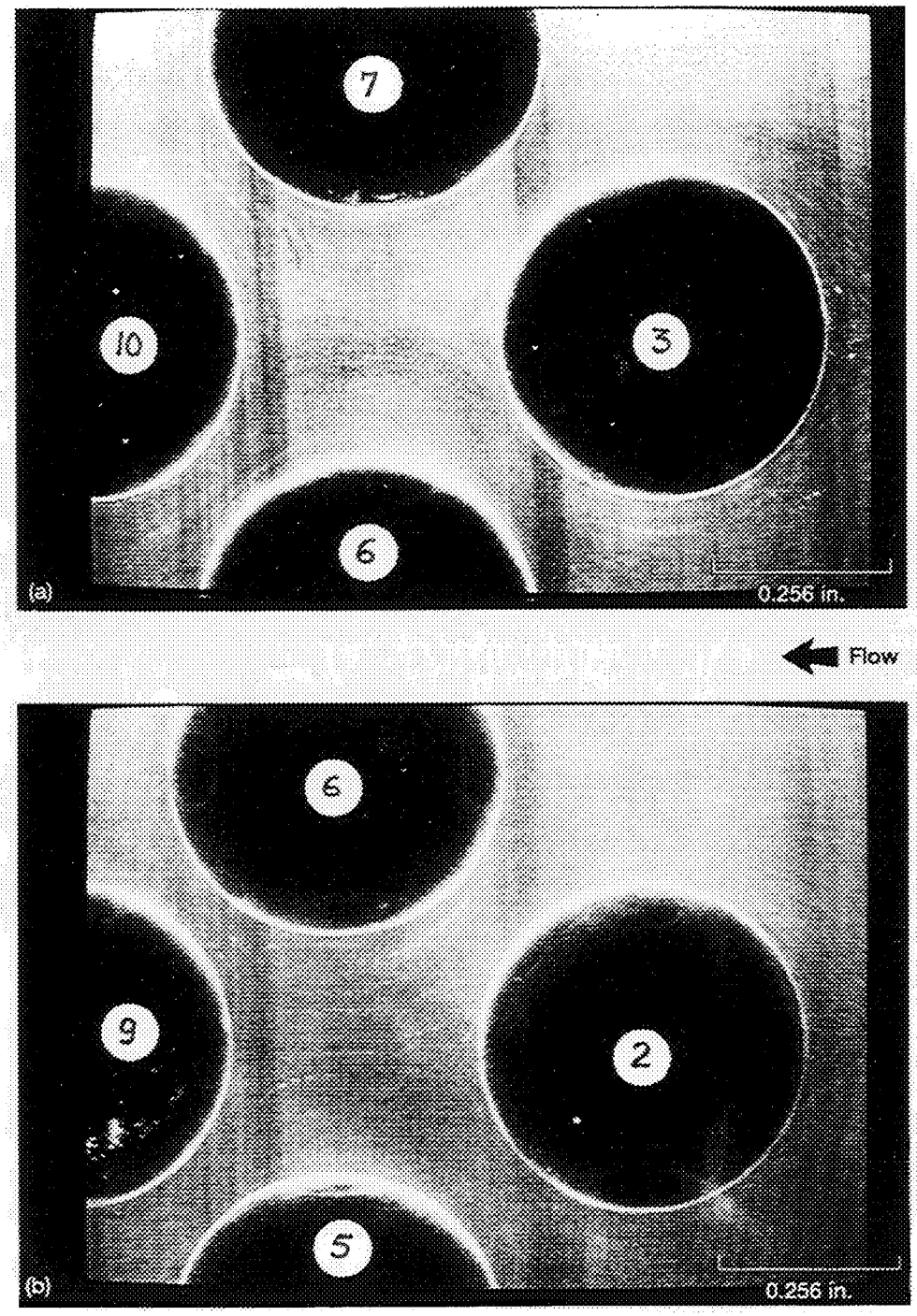

Figure 7.—Details of flow in the front two columns (1, 2), see also figure 10. (a) Spheres 3, 6, 7, 10. (b) Spheres 2, 5, 6, 9.

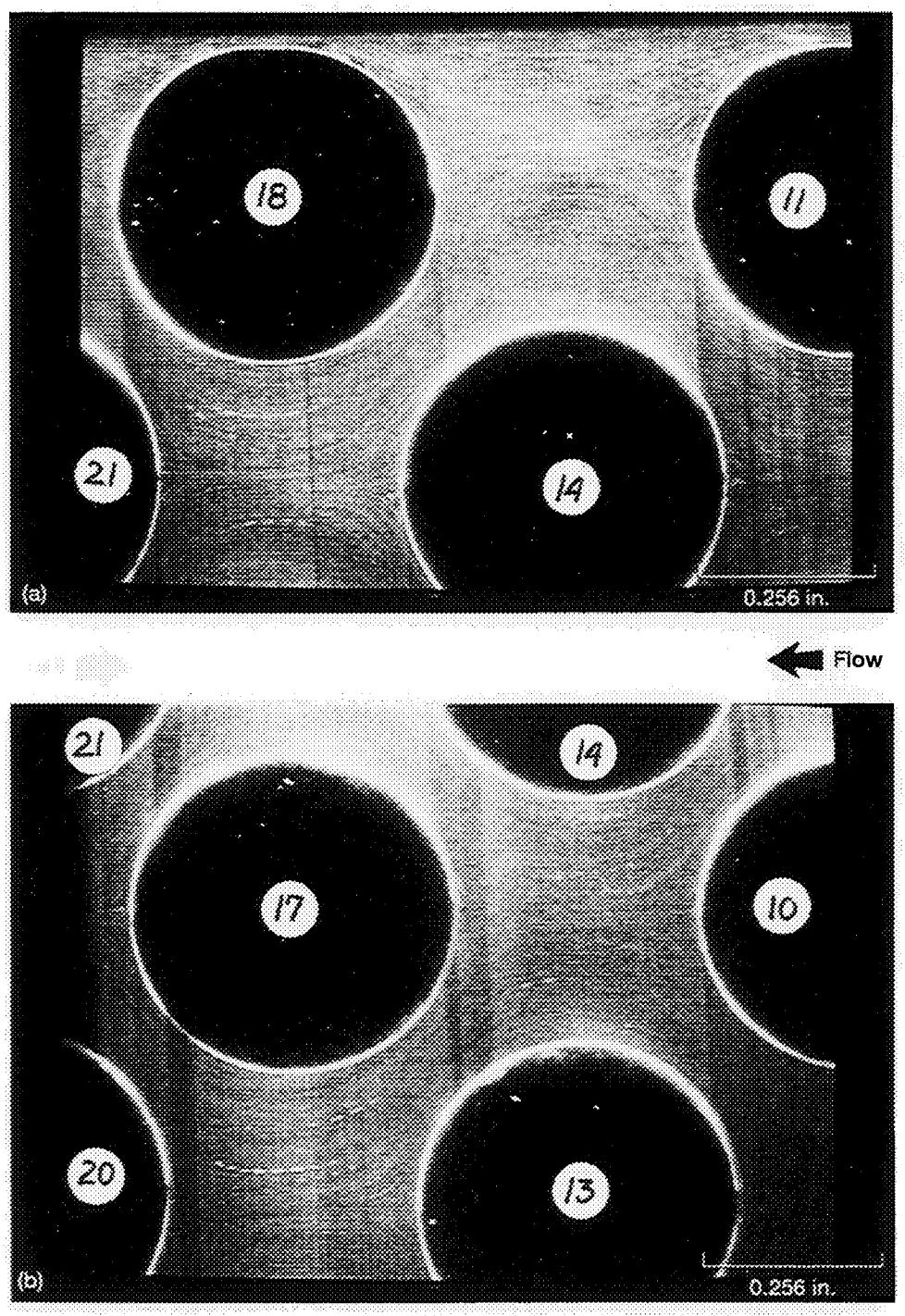

Figure 8.—Details of flow in the middle three columns (3, 4, 5), see also figure 10. (a) Spheres 11, 14, 18, 21. (b) Spheres 10, 13, 14, 17, 20, 21.

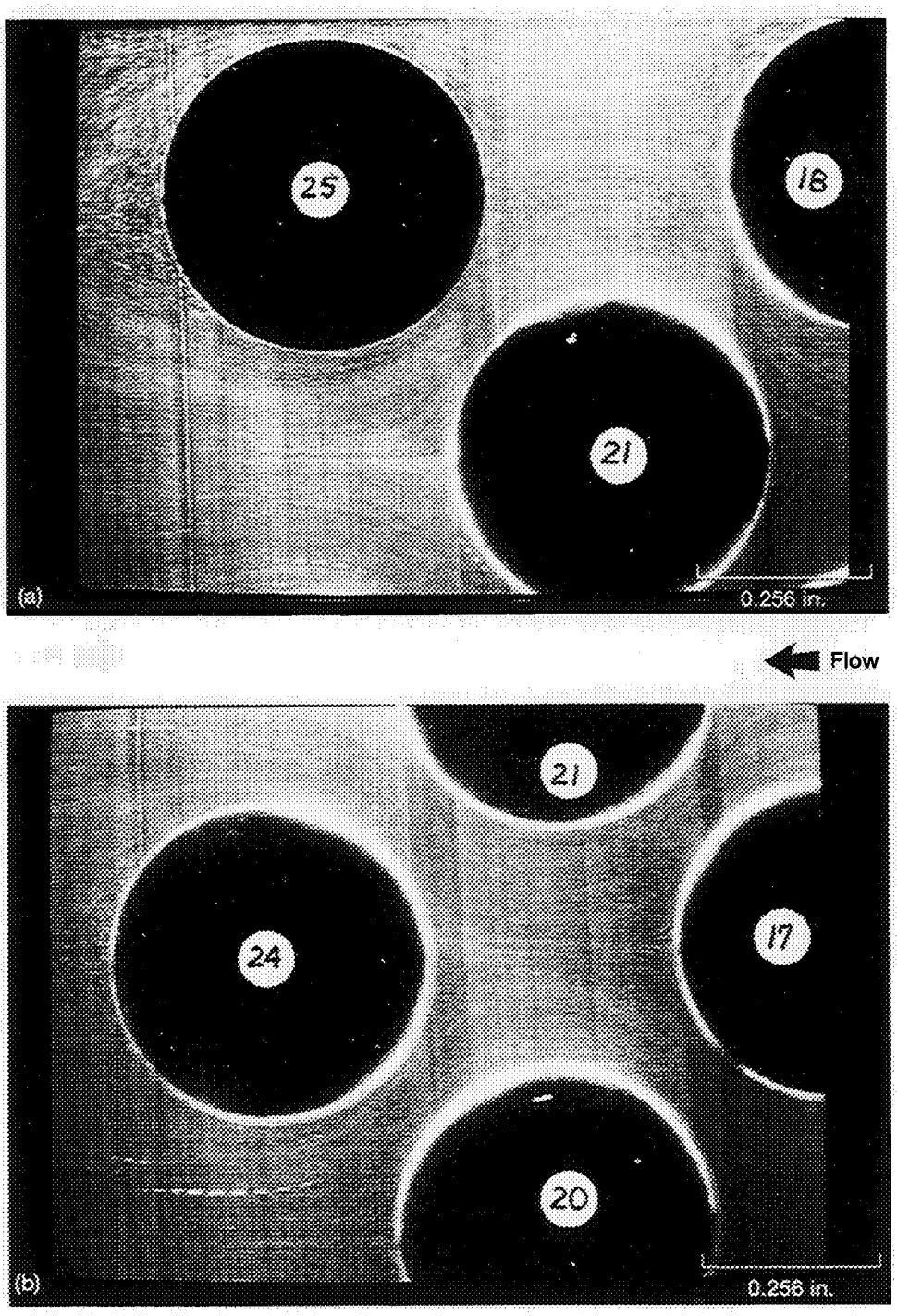

Figure 9.—Details of flow in the last two columns (6, 7), see also figure 10. (a) Spheres 18, 21, 25. (b) Spheres 17, 20, 21, 24.

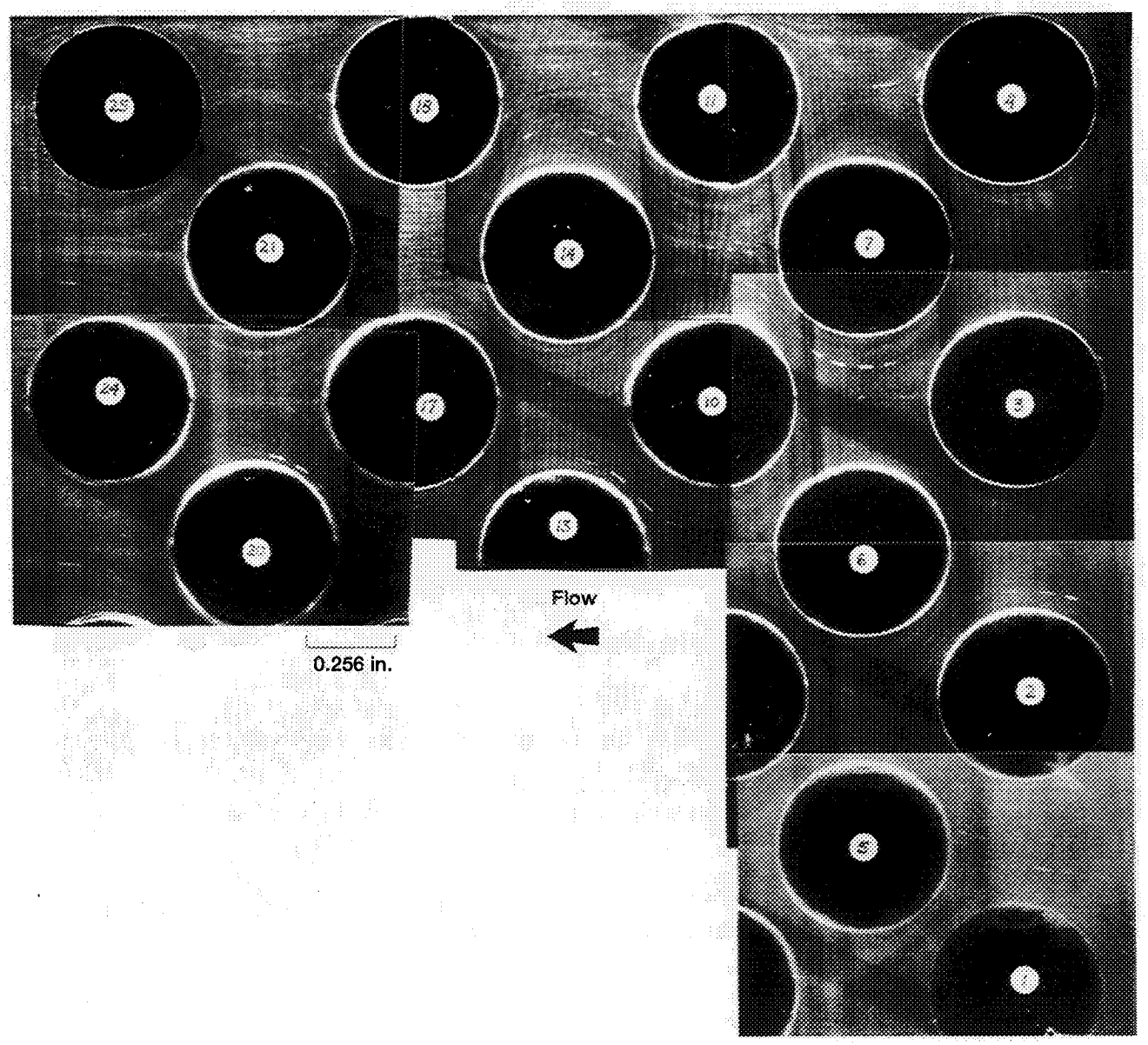

Figure 10.—Visualization of flow in a 12.7 mm diameter sphere matrix (figure 4), 6.4 mm from front wall (z = 1.0); flow at 3.0 GPM.

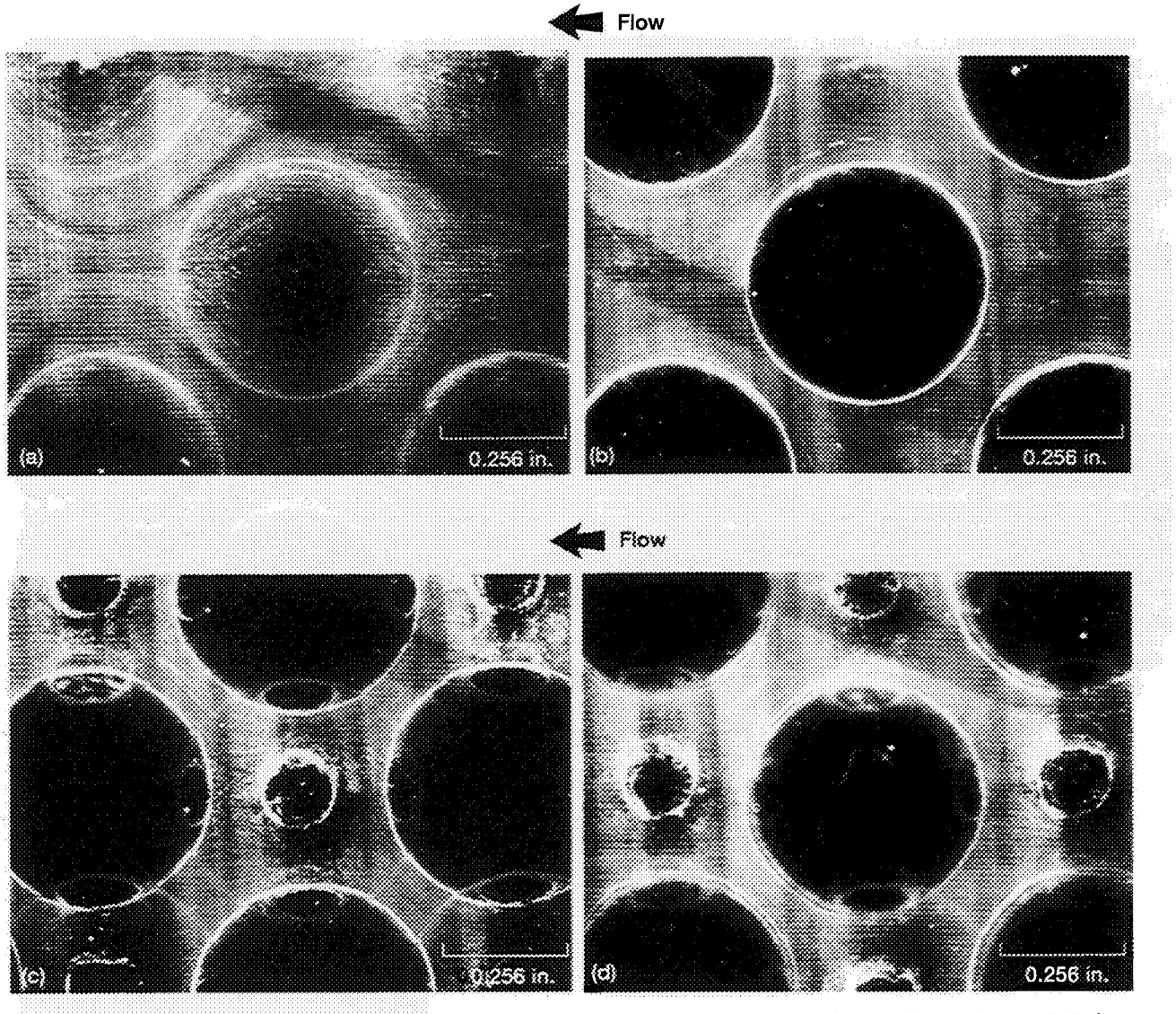

Figure 11.—Transverse visualization of flow in a 12.7 mm diameter sphere matrix (figure 4), at columns 4, 5, 6; flow at 3.0 GPM. (a) z = 0, front wall. (b) z = 1, 0.5 sphere diameters from wall. (c) z = 2, 1.0 sphere diameters from wall. (d) z = 3, 1.5 sphere diameters from wall.

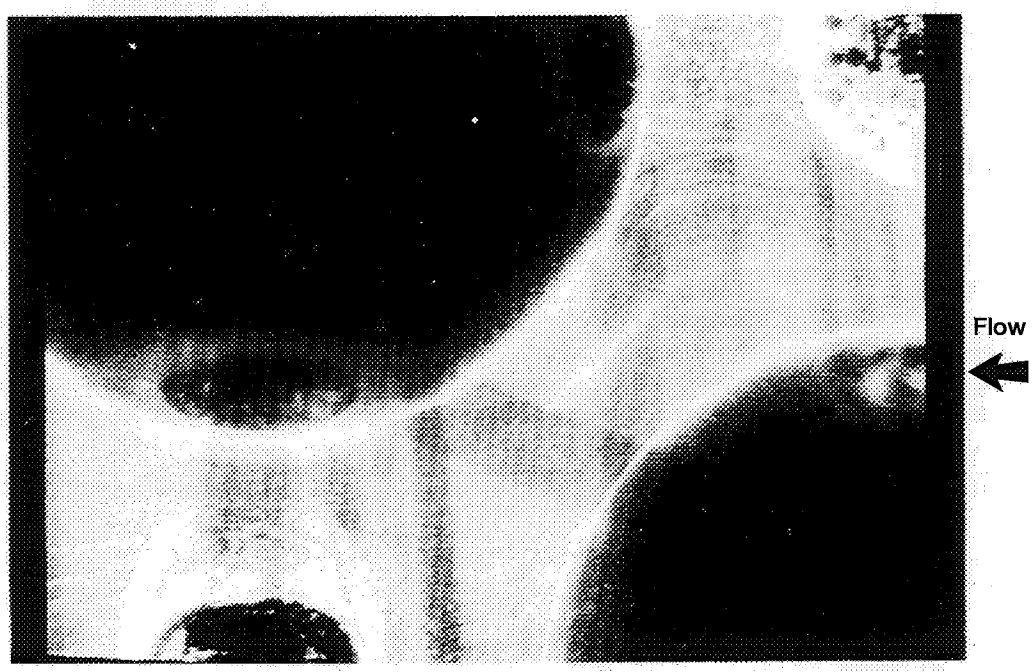

Figure 12.—Sphere matrix flow image at 7.8X, 12.7 mm diameter, 3.0 GPM.

REPORT DOCUMENTATION PAGE

Form Approved
OMB No. 0704-0188

1. AGENCY USE ONLY (*Leave blank*)	2. REPORT DATE	3. REPORT TYPE AND DATES COVERED
	January 1997	Technical Memorandum

4. TITLE AND SUBTITLE

Experimental Visualization of Flows in Packed Beds of Spheres

5. FUNDING NUMBERS

WU–233–1B–1B

6. AUTHOR(S)

R.C. Hendricks, S. Lattime, M.J. Braun, and M.M. Athavale

7. PERFORMING ORGANIZATION NAME(S) AND ADDRESS(ES)

National Aeronautics and Space Administration
Lewis Research Center
Cleveland, Ohio 44135–3191

8. PERFORMING ORGANIZATION REPORT NUMBER

E–10527–1

9. SPONSORING/MONITORING AGENCY NAME(S) AND ADDRESS(ES)

National Aeronautics and Space Administration
Washington, DC 20546–0001

10. SPONSORING/MONITORING AGENCY REPORT NUMBER

NASA TM–107365

11. SUPPLEMENTARY NOTES

Prepared for the First Pacific Symposium on Flow Visualization and Image Processing sponsored by the Pacific Center of Thermal-Fluids Engineering, Honolulu, Hawaii, February 23–26, 1997. R.C. Hendricks, NASA Lewis Research Center; S. Lattime, B&C Engineering, Akron, Ohio 44325; M.J. Braun, University of Akron, Akron, Ohio 44325; and M.M. Athavale, CFD Research Corporation, Huntsville, Alabama 35805 . Responsible person, R.C. Hendricks, organization code 5800, (216) 977–7507.

12a. DISTRIBUTION/AVAILABILITY STATEMENT

Unclassified - Unlimited
Subject Categories 07 and 20

This publication is available from the NASA Center for AeroSpace Information, (301) 621–0390.

12b. DISTRIBUTION CODE

13. ABSTRACT (*Maximum 200 words*)

The flow experiment consisted of an oil tunnel, 76mm x 76 mm in cross section, packed with lucite spheres. The index of refraction of the working fluid and the spheres were matched such that the physical spheres invisible to the eye and camera. By seeding the oil and illuminating the packed bed with planar laser light sheet, aligned in the direction of the bulk flow, the system fluid dynamics becomes visible and the 2-D projection was recorded at right angles to the bulk flow. The planar light sheet was traversed from one side of the tunnel to the other providing a simulated 3-D image of the entire flow field. The boundary interface between the working fluid and the sphere rendered the sphere black permitting visualization of the exact locations of the circular interfaces in both the axial and transverse directions with direct visualization of the complex interstitial spaces between the spheres within the bed. Flows were observed near the surfaces of a plane and set of spheres as well as minor circles that appear with great circles and not always uniformly ordered. In addition to visualizing a very complex flow field, it was observed that flow channeling in the direction of the bulk flow occurs between sets of adjacent spheres. Still photographs and video recordings illustrating the flow phenomena will be presented.

14. SUBJECT TERMS	15. NUMBER OF PAGES
Porous media; Packed beds; Flow visualization; Spheres	15
	16. PRICE CODE: A03

17. SECURITY CLASSIFICATION OF REPORT	18. SECURITY CLASSIFICATION OF THIS PAGE	19. SECURITY CLASSIFICATION OF ABSTRACT	20. LIMITATION OF ABSTRACT
Unclassified	Unclassified	Unclassified	